Advances in Machinery, Materials Science and Engineering Application
M. Chen et al. (Eds.)

doi:10.3233/ATDE220442

LaB_6 as a Functional Separator Modifier for Improved Lithium Sulfur Batteries

Tong ZHANG [a], Biao JIN [a], Zhenzhen LI [a], Chaoda CHEN [a,1]
[a] *Guangdong University of Science and Technology, Dongguan 523000, China*

Abstract. Metal borides have excellent chemical and electrochemical stability, high electrochemical sensitivity, and abundant active sites. According to experiments, metal borides can greatly reduce the shuttle effect in lithium-sulfur batteries and boost their electrochemical performance when used as sulfur host materials. In this thesis, we use polar lanthanum boride materials as materials for lithium-sulfur batteries that modify separators, and take advantage of its strong chemical bonding with polar polysulfides to reduce the shuttle effect. The experimental data demonstrate that the polar lanthanum boride can significantly improve the overall reaction kinetic performance as well as cyclic stability of the cell, resulting in excellent electrochemical performance.

Keywords. Lithium-sulfur batteries, separator, shuttle effect, modify

1. Introduction

The potential energy density of a lithium-sulfur battery (2600 Wh kg^{-1}) is substantially higher than that of a lithium-ion battery system since it uses monolithic sulfur as the cathode material and lithium as the anode material (420 Wh kg^{-1}) [1-4]. In addition, the high abundance of sulfur cathode, the cost is much lower than that of lithium-ion battery cathode materials such as $LiCoO_2$, etc. Moreover, sulfur is not polluting to the environment, which is in line with the current important strategy of sustainable development and has a bright future for commercial application. However, there are still some problems in the lithium-sulfur battery system that need to be solved [5, 6].

As a crucial part in the battery structure, the membrane plays an important role of separating the positive and negative electrodes, avoiding the internal transfer of electrons caused by direct contact between them, and conducting ions [7, 8]. Currently, the Celgard separator used in the lithium-sulfur battery system is not specifically designed for the lithium-sulfur battery system, the separator aperture size is large, resulting in the provision of ion channels at the same time, the liquid phase polysulfide dissolved in the electrolyte also through the holes in the separator into the negative side, The shuttle effect is another name for this process, which causes the battery's electrochemical performance to degrade [9-12]. Therefore, functional modification of the separator to enable it to physically or chemically restrain the passage of polysulfides becomes the most effective strategy to suppress the shuttle effect [13-16].

---

[1] Chaoda Chen, Corresponding Author, College of Mechanical and Electrical Engineering, Guangdong University of Science and Technology, Dongguan, China; E-mail: zt18143095811@163.com.

LaB_6 is chosen to modify the lithium-sulfur battery separator, and the experimental data proved that polar LaB_6 can greatly enhance the battery's cycle stability and reaction kinetics, so that the battery obtained excellent electrochemical performance [17-19].

2. Experimental Section

2.1. Chemical Reagents and Experimental Materials

The names, specifications and manufacturer information of some of the key materials utilized in this investigation are listed in table 1.

Table 1. Chemical reagents and experimental materials.

Name	Specification	Manufacturer
Lanthanum hexaboride (LaB6)	99.9%	Macklin
Monomeric sulfur (S)	Battery Grade	Sigma-Aldrich
Multi-walledcarbon nanotubes (CNT)	95%	Xianfeng Nano
Lithium sulfide (Li2S)	Battery Grade	Sigma-Aldrich

2.2. Preparation of Materials Methods

(1) Preparation of S@CNT composites by hot-melt method: S and CNT were blended at a mass ratio of 3:1 in a mortar, and anhydrous ethanol was added and ground until the ethanol evaporated, and the mixture was repeated three to four times to make it homogeneous.

(2) Preparation of positive materials: S@CNT composite, Super P and Polyvinylidene Fluoride (PVDF) were weighed at a weight ratio of 7:2:1 and placed in a mortar, followed by the addition of an appropriate amount of NMP for grinding until the slurry was homogeneous. Using a squeegee, the slurry was put on clean aluminum foil and allowed to dry for a whole night at 60 °C in a vacuum oven. A poles die was used to flatten the poles into 1 cm diameter discs with a sulfur loading of roughly 1.2 mg cm^{-2}.

(3) Separator modification method: LaB_6, Super P and PVDF are evenly mixed in a mortar at a mass ratio of 8:1:1, and NMP is introduced for grinding until the slurry is uniform. After that, the slurry is evenly coated on the clean PP diaphragm with a scraper, then dried overnight in a vacuum oven at 60 °C. The septa were pressed into 1.8 cm diameter discs using a mold, and the unit area loading of LaB_6 was about 0.8 mg cm^{-2}.

(4) Preparation of 0.02 M Li_2S_6 solution: In a glove box, DOL and DME were mixed uniformly in a volume ratio of 1:1, S and Li_2S (molar ratio of 5:1) were added and placed on a magnetic stirring table at 50 °C for 12 h to form a uniform yellow solution.

2.3. Electrochemical Test

In this experiment, 2032 button cells were used for electrochemical testing of the materials, and the battery assembly process was performed in Ar atmosphere glove box, and the battery testing conditions were all at room temperature (25°C).The positive electrode was covered with S@CNT composite material, and the negative electrode was lithium metal. Celgard 2400 PP film and LaB6 modified PP diaphragm as the diaphragm. Configure DOL/DME electrolyte with 1.0 M LiTFSI (volume ratio 1:1) and add LiNO3 with 2% mass fraction as additive. The battery was charged and discharged at constant current using a Land-2100 battery tester in the voltage range of 1.7-2.8 V. Within this voltage range, the battery was subjected to cyclic voltammetric curve (CV) testing (0.1 mV s^{-1}) using a Bio-Logic VSP multichannel electrochemical workstation.

3. Results and Discussion

3.1. Morphological Analysis

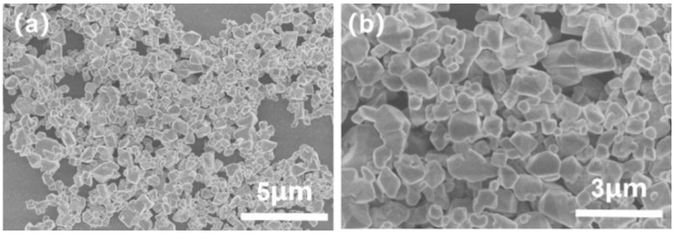

Figure 1. SEM image of LaB$_6$.

As shown in figure 1 (a), we observed the microscopic morphology of LaB$_6$ using SEM, which is an irregular bulk powder with particle size ranging from 1 to 3 μm. Further enlarging the SEM scale magnification as shown in figure 1 (b), we can find that LaB6's surface is evidently rather smooth and devoid of pore structure.

3.2. Electrochemical Performance

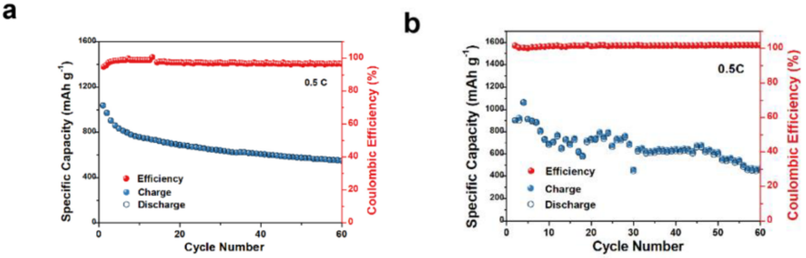

Figure 2. Cycling performance of cells equipped with (a) LaB$_6$-modified separator and (2) PP separator at 0.5 C current density.

The performance of the betters with the modified diaphragms of LaB$_6$ was then investigated and contrasted with the performance of the cell without the modified diaphragms. As shown in figures 2(a) and 2(b), the specific capacity of the first cycle for the battery with LaB$_6$ modified separator was 1036 mAh g^{-1} at 0.5 C, and after 60 cycles, the specific capacity maintained at 550 mAh g^{-1}, and the Coulomb efficiency was always close to 100%. The comparison group without separator modification was extremely unstable, with a wide range of capacity fluctuations within the initial 30 cycles and only 450 mAh g^{-1} remaining after 60 cycles.

The multiplicative performance tests of the battery are displayed in figure 3 at 0.2, 0.5, 1, 2, 1, and 0.5 C current densities, respectively, and the data show that the average discharge capacity of the battery per turn is 1150, 810, 680, 600, 630, and 670 mAh g^{-1}, and the multiplicative performance of the battery after separator modification also performs well.

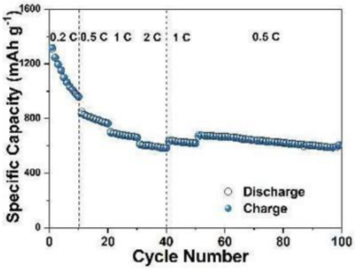

Figure 3. Rate performance of LaB$_6$-modified separators at various current densities.

We also performed CV measurements on the cell using LaB$_6$ modified separator with a voltage range of 1.7-2.8 V and a sweep rate of 0.1 mV s^{-1}. The first five cycles of CV curves are shown in figure 4, the CV curves is divided into two parts, the lower part shows the discharging process of the cell with two obvious reduction peaks. The one reduction peak at a high potential corresponds to the process by which S8 is converted to long chains of polysulfide, and the other to the process by which long chains of polysulfide are converted to short chains of polysulfide. The upper part represent the charging process of the cell, and the two oxidation peaks represent the short-chain polysulfides can change into long-chain polysulfides in a reversible manner [20-22]. The battery's CV curves may be seen to recur consistently between the second and fifth cycles, demonstrating the battery's good cycle stability.

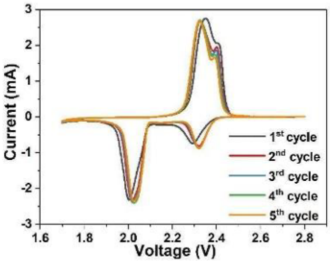

Figure 4. CV curves at 1 C of s of the first five cycles for cell with LaB$_6$ separator.

To avoid the possibility of LaB$_6$ capacity contribution in the lithium-sulfur battery's operational voltage range, which affects the analysis of the battery electrochemical performance, we also assembled LaB$_6$/Li half-cells, replacing sulfur with LaB$_6$ as the battery cathode active material, lithium sheet as the negative electrode, and PP film as the separator, and performed electrochemical tests (figure 5), and the results showed that in the lithium-sulfur battery operating voltage range (1.7-2.8 V), LaB$_6$ has almost no capacity contribution and does not affect the assessment of the battery capacity, which indicates that LaB$_6$ has good electrochemical compatibility in lithium-sulfur batteries and will be stable during the electrochemical reaction of the battery.

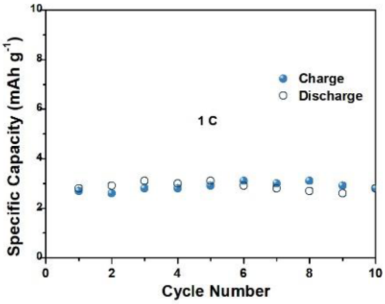

Figure 5. Cyclic performance of LaB$_6$ /Li half cell.

It can be visually seen from the above data that the LaB$_6$ modified separator resulted in a large increase in the charge/discharge capacity for the cell and significantly improved the cycle stability for the battery, causing the battery's electrochemical performance to significantly improve.

4. Conclusion

In this paper, Lithium-sulfur battery separators are modified using LaB6, firstly, it is characterized structurally and morphologically, then it is analyzed electrochemically, and the reasons of the enhancement of the electrochemical performance for the cell are investigated, and the following conclusions are obtained. Second, the significant chemisorption of polysulfide with LaB6 can successfully prevent the polysulfide from traveling through the separator, reduce the contact with the lithium cathode, and prevent the occurrence of side reactions, thus effectively binding the active material to the cathode side, avoiding irreversible loss of battery capacity and elevating the overall cycling stability of the battery.

Acknowledgements

The funding support for this project came from the Research of Dongguan Science and Technology of Social Development Program (No.20211800905482); Scientific Research Project of Guangdong University of Science and Technology (No. GKY-2021KYZDK-4); Project of Characteristic Innovation of Guangdong Province (No.2021KTSCX148); 2021 Teaching Quality and Teaching Reform Project of Undergraduate Colleges and Universities in Guangdong Province (Yue Jiao Gao Han [2021] No. 29); Dongguan Sci-tech Commissoner Program (No.20201800500592; No.20201800500622);

References

[1] Qiu W, An C, Yan Y, Xu J, Zhang Z, Guo W, Wang Z, Zheng Z, Wang Z and Deng Q. Journal of Power Sources. 2019; 423: 98-105.

[2] Lei T, Chen W, Lv W, Huang J, Zhu J, Chu J, Yan C, Wu C, Yan Y and He. Joule. 2018; 2: 2091-2104.

[3] Manthiram A, Fu Y, Chung SH, Zu C and Su YS. Chemical Reviews. 2014; 114: 11751-11787.

[4] Fan X, Sun W, Meng F, Xing A and Liu J. Green Energy & Environment. 2018; 3: 2-19.

[5] Zheng Y, Zheng S, Xue H and Pang H. Journal of Materials Chemistry A. 2019; 7: 3469-3491.

[6] Jiang Y, Chen F, Gao Y, Wang Y, Wang S, Gao Q, Jiao Z, Zhao B and Z. Chen. Journal of Power Sources. 2017; 342: 929-938.

[7] Pei F, Lin L, Fu A, Mo S, Ou D, Fang X and Zheng N. Joule. 2018; 2: 323-336.

[8] Hsieh YY, Zhang L, DeArmond D, Kanakaraj SN, Adusei PK, Alvarez NT, Fang Y, Daum J and Shanov V. Carbon. 2018; 139: 1093-1103.

[9] Lu H, Guo Q, Fan Q, et al. Journal of Alloys and Compounds. 2021; 870: 159341.

[10] Li F, Zhang X, Liu X and Zhao M. ACS Applied Materials & Interfaces. 2018; 10: 15012-15020.

[11] Jeong YC, Kim JH, Nam S, Park CR and Yang SJ. Advanced Functional Materials. 2018; 28: 1707411.

[12] Huang S, Huixiang E, Yang Y, Zhang Y, Ye M and Li CC. Journal of Materials Chemistry A. 2021; 9: 7458-7480.

[13] Abbas SA, Ding J, Wu SH, Fang J, et al. ACS Nano. 2017; 11: 12436-12445.

[14] Ghazi ZA, He X, Khattak AM, et al. Advanced Materials. 2017; 29: 1606817.

[15] Liu XC, Zhou SP, Liu M, et al. Nano Energy. 2018; 50: 685-690.

[16] Jin L, Ni J, Shen C, Peng F, et al. Journal of Power Sources. 2020; 448: 227336.

[17] Yu Y, Wang S, Li W and Chen Z. Powder Technology. 2018; 323: 203-207.

[18] Li S, Zhang W, Zheng J, Lv M, Song H and Du L.,Advanced Energy Materials. 2021; 11: 2000779.

[19] Guan B, Zhang Y, Fan L, Wu X, Wang M, Qiu Y, Zhang N and Sun K. ACS Nano,. 2019; 13: 6742-6750.

[20] Liu B, Huang S, Kong D, Hu J and Yang HY. Journal of Materials Chemistry A. 2019; 7: 7604-7613.

[21] Cai J, Fan Z, Jin J, Shi Z, Dou S, Sun J and Liu Z. Nano Energy. 2020; 75: 104970.

[22] Mahankali K, Thangavel NK, Gopchenko D and Arava LMR. ACS applied Materials & Interfaces. 2020; 12: 27112-27121.